

NUMERICAL STUDIES OF STOCHASTIC RESONANCE

MICHAEL V. TRETYAKOV

WIAS, Mohrenstr. 39, 10117 Berlin
Ural State University, Lenin str. 51, 620083 Ekaterinburg, Russia
e-mail: Michael.Tretyakov@usu.ru

submitted: 12th March 1997

1991 *Mathematics Subject Classification.* 65C20, 60H10.

Key words and phrases. stochastic differential equations, numerical methods, stochastic resonance.

ABSTRACT. A new numerical technique is proposed to study the stochastic resonance (SR) phenomenon. The proposed numerical approach allows to find characteristics of SR faster than the previous ones. The signal-to-noise ratio and phase shifts for a system of noisy coupled oscillators are simulated. The spatiotemporal synchronization is shown by means of trajectory analysis.

1. INTRODUCTION

The term "stochastic resonance" (SR) is historically used in connection with a variety of effects attributable to the interaction between a periodic applied force and noise in nonlinear systems. SR was first considered in the context of the earth's ice ages [1], then observed in lasers [2], applied to sensory neurophysiological and brain function problems [3, 4], demonstrated in experiments with a bistable superconducting quantum interference device [5]. Attempts to exploit SR for technological advantage are one of the main trends in current research on this topic. As a survey on SR, one can use the proceedings of workshops [6, 7] or the review [8]. A more comprehensive and actual list of references is also possible to find at the Web site [9].

In recent papers [10, 11, 12] the authors investigate SR in large arrays (up to 512 elements) of noisy coupled oscillators. The phenomenon was named in [10] as array enhanced stochastic resonance (AESR). It was shown that additionally to common features of SR, AESR demonstrates a spatiotemporal synchronization and there is an additional design parameter - the coupling strength, which essentially affects the behavior of SR characteristics. The experimental evidence of the AESR phenomenon was reported in [13], where it was shown that the signal-to-noise ratio of the output signal of a single diode resonator can be significantly improved by coupling it diffusively into an array of resonators. The spatiotemporal synchronization was also experimentally confirmed. The authors marked [10, 11, 13] that the AESR phenomenon may find its further applications in neural dynamics and in the area of signal processing. AESR was studied analytically in some limit cases [14, 11], but the basic tool for its investigation is numerical simulation of a system of stochastic differential equations (SDE).

To calculate the characteristics describing SR, one must integrate the system on long time intervals and simulate a sufficiently large number of independent realizations. Main characteristics of SR (e.g., signal-to-noise ratio) are expectations of functionals of SDE solution. As is known [15, 16, 17, 18], weak numerical methods are sufficient to calculate such quantities and are quite simple for realization and efficient. Special powerful weak numerical methods for SDE with relatively small noise were proposed in [19]. The effects of SR can usually be observed under small noise, and one can believe that the methods of Ref. [19] may be a good tool for studying the SR phenomenon. The first tests with one-dimensional Stratonovich equation, describing the multiplicative stochastic resonance in optical bistable system [20], gave good results [19]. Here we apply these methods and propose a numerical technique to study the SR phenomenon. The proposed numerical approach allows us to study properties of SR faster than the previous ones.

The paper is organized as follows. The numerical technique for calculating the signal-to-noise ratio and phase shifts is proposed in Section 2. Section 3 contains numerical results for the array of noisy coupled oscillators. We consider the technique on a simple model, but it is also valid for more complicated systems.

2. DESCRIPTION OF THE NUMERICAL TECHNIQUE

Following Refs. [10, 11], we consider the system

$$dX^{(i)} = [aX^{(i)} - bX^{(i)3} + A \sin(\Omega t + \varphi) + c(X^{(i+1)} - 2X^{(i)} + X^{(i-1)})]dt + \varepsilon dW_i(t)$$

$$(2.1) \quad i = 1, 2, \dots, n, X^{(0)} \equiv X^{(1)}, X^{(n+1)} \equiv X^{(n)}, X(0) = X_o, t \in [0, T]$$

where $X = (X^{(1)}, X^{(2)}, \dots, X^{(n)})$ is an n -dimensional vector, W_i , $i = 1, \dots, n$, are independent standard Wiener processes. The system (2.1) describes a one-dimensional array (chain) of over-damped driven nonlinear oscillators coupled linearly to their nearest neighbors. To ensure a bistable potential (two-state points), a and b must be positive. The phase φ is taken as a uniformly distributed random variable on the interval $[0, 2\pi]$, and the coupling parameter $c \geq 0$.

Let us remind of some definitions of the theory of random processes, which are used below.

A random process $\xi(t)$, $\xi(t) \in R^n$, $t \geq t_o$, is a stationary process [21, 22] if it has two first moments $E\xi(t)$, $E|\xi(t)|^2$ and

$$(2.2) \quad \begin{aligned} E\xi(t) &= E\xi(t + \tau) = \text{const} \\ \text{cov}(\xi(t), \xi(s)) &= \text{cov}(\xi(t + \tau), \xi(s + \tau)) \quad \text{for any } t, s, \text{ and } \tau \end{aligned}$$

where $\text{cov}(\xi(t), \xi(s))$ is the covariation matrix:

$$\text{cov}(\xi(t), \xi(s)) = E\xi(t)\xi(s)^T - E\xi(t)E\xi(s)^T.$$

A random process $\xi(t)$ is a periodic one with a period T_o [21] if

$$(2.3) \quad \begin{aligned} E\xi(t) &= E\xi(t + T_o) \\ \text{cov}(\xi(t), \xi(s)) &= \text{cov}(\xi(t + T_o), \xi(s + T_o)) \quad \text{for any } t, s. \end{aligned}$$

In accordance with Theorem 5.2 and the examples 1, 3 of Ch. 3, § 5 of Ref. [21], there is a solution $X(t)$ of the system (2.1) at each fixed φ , which is a periodic markovian process with the period $2\pi/\Omega$. The periodic process can be converted into a stationary one by the following shift of time [23, 21]: if θ is a random variable, distributed uniformly on $[0, 2\pi/\Omega]$ and independent on $X(t)$, the process $\eta(t) = X(t + \theta)$ is stationary. So, there is a stationary solution $X(t)$ of the system (2.1) in the case of uniformly distributed on $[0, 2\pi]$, independent on $X(t)$ random phase φ .¹ Due to Theorem 7.1 of Ref. [21, Ch. 4], there is the unique stationary markovian process $X(t)$ corresponding to the system (2.1), and the solutions of (2.1) under any initial distribution of X_o converge to this stationary process in the weak sense as $t \rightarrow \infty$.²

Let us consider a constituent oscillator of the chain, e.g., the middle one, described by (2.1). Below we shall denote a constituent component (oscillator) $X^{(l)}$, $l \in \{1, 2, \dots, n\}$, of the vector $X(t) \equiv (X^{(1)}, \dots, X^{(n)})$ by $X_c(t)$ and its correlation function by $K(\tau)$ ($K(\tau) = EX_c(t)X_c(t + \tau) - m^2$, $m = EX_c(t)$).

If one converts a periodic process with the period $2\pi/\Omega$ into a stationary one by the above described time shift, the correlation function of the stationary process has the following form [23]

$$(2.4) \quad K(\tau) = K_o(\tau) + 2 \sum_{k=1}^{\infty} \alpha_k \cos k\Omega\tau.$$

¹The physical background to use such a distribution of the phase φ can be found, e.g. in [24, 8].

²The conditions of Theorem 7.1 contain a requirement on process $X(t)$ to be recurrent. The fulfilment of the requirement follows from Lemma 8.1 and the example 3 of Ref. [21, Ch. 3, § 8].

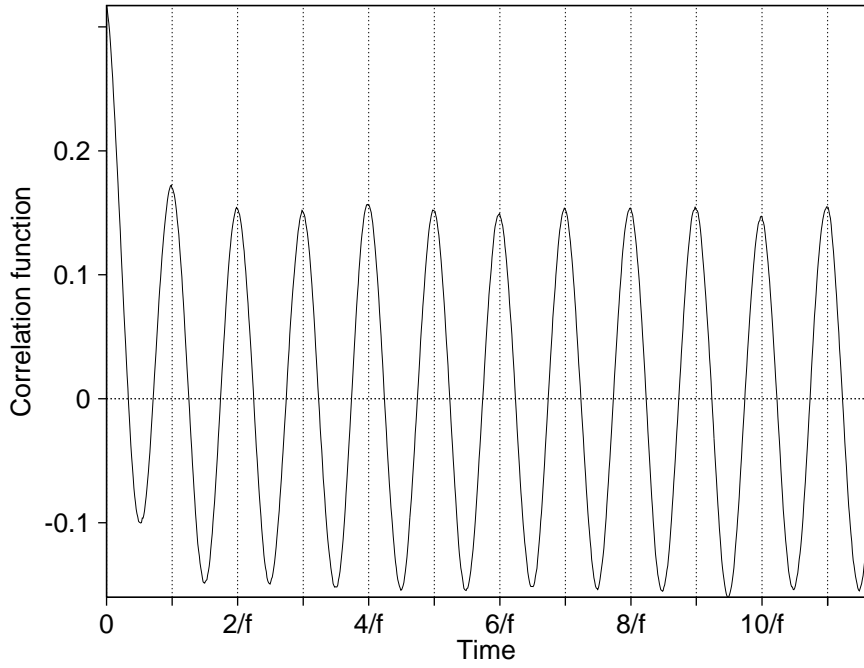


FIGURE 1. The correlation function $K(\tau)$ of the middle oscillator from the array of nine oscillators described by (2.1) under the parameters: $a = 2.1078$, $b = 1.4706$, $A = 1.3039$, $\Omega = 0.7301$, $c = 0.5$, $\varepsilon = 0.5$, $f = \Omega/2\pi$, $T_s = 3/f$, and simulated by (2.7) with $h = 0.1$. The Monte Carlo error is less than 0.0056.

In our case $K_o(\tau)$ goes fast to zero and $\alpha_k = 0$ for even k . Figure 1 demonstrates the behavior of the correlation function for the constituent component of system (2.1). According to the definition, the spectral function $F(\omega)$ can be written as

$$F(\omega) = \frac{1}{\pi} \int_0^{\infty} K(\tau) \frac{\sin \omega \tau}{\tau} d\tau, \quad \omega \in [0, \infty)$$

Using the properties of $K(\tau)$, we have

$$F(\omega) = F_o(\omega) + \sum_{k=1}^{\infty} \alpha_{2k-1} \chi(\omega - (2k-1)\Omega)$$

where

$$F_o(\omega) = \frac{1}{\pi} \int_0^{\infty} K_o(\tau) \frac{\sin \omega \tau}{\tau} d\tau, \quad \chi(x) = \begin{cases} 0, & x < 0 \\ 1/2, & x = 0 \\ 1, & x > 0 \end{cases}$$

And the spectral density $S(\omega)$ is equal to

$$(2.5) \quad S(\omega) = S_o(\omega) + \sum_{k=1}^{\infty} \alpha_{2k-1} \delta(\omega - (2k-1)\Omega),$$

$$(2.6) \quad S_o(\omega) = \frac{dF_o(\omega)}{d\omega} = \frac{1}{\pi} \int_0^{\infty} K_o(\tau) \cos \omega \tau d\tau$$

So, as it is generally known, the spectrum $S(\omega)$ for a system like (2.1) consists of a broadband noise background and δ -function spikes at frequencies $\omega = (2k-1)\Omega$, $k = 1, 2, \dots$.

2.1. Numerical method. Let us introduce an equidistant discretization Δ_N of the interval $[0, T]$: $\Delta_N = \{t_i : i = 0, 1, \dots, N; 0 = t_0 < t_1 < \dots < t_N = T\}$; the time step $h = t_{i+1} - t_i$.

To simulate the system (2.1), which is a system with additive noises, we take the weak full Runge-Kutta method with the error $O(h^4 + \varepsilon^4 h^2)$ from Ref. [19]. In the case of the system (2.1) the method has the form

$$\begin{aligned} X_{k+1}^{(i)} &= X_k^{(i)} + \varepsilon h^{1/2} \xi_k^{(i)} + \left(k_1^{(i)} + 2k_2^{(i)} + 2k_3^{(i)} + k_4^{(i)} \right) / 6 + \varepsilon h^{3/2} a \eta_k^{(i)} \\ &- hb \left((X_k^{(i)} + \varepsilon h^{1/2} \eta_k^{(i)})^3 - (X_k^{(i)} - \varepsilon h^{1/2} \eta_k^{(i)})^3 \right) / 2 + \varepsilon h^{3/2} c \left(\eta_k^{(i+1)} - 2\eta_k^{(i)} + \eta_k^{(i-1)} \right), \end{aligned} \quad (2.7)$$

$i = 1, \dots, n, k = 0, 1, \dots, N$

where $(X_k^{(1)}, X_k^{(2)}, \dots, X_k^{(n)}) = X_k = \bar{X}(t_k)$ is the approximation of a solution $X(t_k)$ of the system (2.1),

$$\begin{aligned} k_1^{(i)} &= h \left(a X_k^{(i)} - b X_k^{(i)3} + A v_k + c \left(X_k^{(i+1)} - 2X_k^{(i)} + X_k^{(i-1)} \right) \right), \\ k_2^{(i)} &= h \left(a \left(X_k^{(i)} + k_1^{(i)} / 2 \right) - b \left(X_k^{(i)} + k_1^{(i)} / 2 \right)^3 + A(v_k + l_1 / 2) \right. \\ &\left. + c \left(\left(X_k^{(i+1)} + k_1^{(i+1)} / 2 \right) - 2 \left(X_k^{(i)} + k_1^{(i)} / 2 \right) + \left(X_k^{(i-1)} + k_1^{(i-1)} / 2 \right) \right) \right), \\ k_3^{(i)} &= h \left(a \left(X_k^{(i)} + \varepsilon h^{1/2} \xi_k^{(i)} + k_2^{(i)} / 2 \right) - b \left(X_k^{(i)} + \varepsilon h^{1/2} \xi_k^{(i)} + k_2^{(i)} / 2 \right)^3 + A(v_k + l_2 / 2) \right. \\ &\left. + c \left(\left(X_k^{(i+1)} + \varepsilon h^{1/2} \xi_k^{(i+1)} + k_2^{(i+1)} / 2 \right) - 2 \left(X_k^{(i)} + \varepsilon h^{1/2} \xi_k^{(i)} + k_2^{(i)} / 2 \right) \right. \right. \\ &\left. \left. + \left(X_k^{(i-1)} + \varepsilon h^{1/2} \xi_k^{(i-1)} + k_2^{(i-1)} / 2 \right) \right) \right), \\ k_4^{(i)} &= h \left(a \left(X_k^{(i)} + \varepsilon h^{1/2} \xi_k^{(i)} + k_3^{(i)} \right) - b \left(X_k^{(i)} + \varepsilon h^{1/2} \xi_k^{(i)} + k_3^{(i)} \right)^3 + A(v_k + l_3) \right. \\ &\left. + c \left(\left(X_k^{(i+1)} + \varepsilon h^{1/2} \xi_k^{(i+1)} + k_3^{(i+1)} \right) - 2 \left(X_k^{(i)} + \varepsilon h^{1/2} \xi_k^{(i)} + k_3^{(i)} \right) \right. \right. \\ &\left. \left. + \left(X_k^{(i-1)} + \varepsilon h^{1/2} \xi_k^{(i-1)} + k_3^{(i-1)} \right) \right) \right) \end{aligned} \quad (2.8)$$

$k_j^{(o)} \equiv k_j^{(1)}, k_j^{(n+1)} \equiv k_j^{(n)}, j = 1, \dots, 4, X_k^{(o)} \equiv X_k^{(1)}, X_k^{(n+1)} \equiv X_k^{(n)}$

Here we simulate $\sin(\Omega t + \varphi)$ of (2.1) by the system

$$\begin{aligned} du &= -\Omega v dt, \\ dv &= \Omega u dt, \end{aligned} \quad (2.9)$$

$$u(0) = u_o = \cos \varphi, v(0) = v_o = \sin \varphi$$

where φ is a random variable distributed uniformly on the interval $[0, 2\pi]$. The system (2.9) is approximated by

$$u_{k+1} = u_k + (m_1 + 2m_2 + 2m_3 + m_4) / 6,$$

$$(2.10) \quad v_{k+1} = v_k + (l_1 + 2l_2 + 2l_3 + l_4) / 6$$

where

$$m_1 = -h\Omega v_k, \quad l_1 = h\Omega u_k, \quad m_2 = -h\Omega (v_k + l_1/2), \quad l_2 = h\Omega (u_k + m_1/2),$$

$$m_3 = -h\Omega (v_k + l_2/2), \quad l_3 = h\Omega (u_k + m_2/2),$$

$$(2.11) \quad m_4 = -h\Omega (v_k + l_3), \quad l_4 = h\Omega (u_k + m_3).$$

We use v_k and l_j , $j = 1, 2, 3$ of (2.10)-(2.11) in the expressions of (2.8).

The mutually independent random variables $\xi_k^{(i)}$ and $\eta_k^{(i)}$ from (2.7)-(2.8) are simulated according to the laws

$$P(\xi = 0) = 2/3, \quad P(\xi = -\sqrt{3}) = P(\xi = \sqrt{3}) = 1/6,$$

$$P(\eta = -1/\sqrt{12}) = P(\eta = 1/\sqrt{12}) = 1/2$$

The method (2.7) has the second order of weak convergence with respect to the time step h . But it usually gives more accurate results (especially under low noise level) and is not essentially more complicated from the computational point of view than a standard weak method of order 2 [15, 16, 17, 18] (see details in [19]). To carry out our experiments, we do not take a more accurate method: a standard method of order 3 or methods with errors $O(h^4 + \varepsilon^6 h^2)$, $O(h^4 + \varepsilon^2 h^3)$, $O(h^4 + \varepsilon^4 h^3)$, etc. of [19], because the method (2.7) ensures enough accuracy and speed of calculations to study SR characteristics in our case and there are no reasons to take a more accurate and, naturally, more complicated method (e.g., there are no full Runge-Kutta schemes among the mentioned more accurate methods).

2.2. Evaluation of the signal-to-noise ratio. One of the main characteristics, describing the SR phenomenon, is the signal-to-noise ratio (SNR). SNR is a commonly used measure of the information content of the response of a system. The remarkable property of the SR phenomenon is the non-monotonic behavior of SNR as a function of noise level. The function has a maximum, and there is a noise level for which the system acts as a selective amplifier in some range of frequencies.

Here we use the following definition of the output SNR, R , for a constituent oscillator:

$$(2.12) \quad R = \frac{\alpha_1}{S_o(\Omega)}$$

where α_1 and $S_o(\Omega)$ are from (2.5), i.e., R is the ratio of the signal power and noise background at the frequency of applied periodic force. The existing in literature distinctions in SNR definition do not lead to qualitatively different results.

Let us take into consideration a sufficiently small interval of frequencies $[\Omega - \Delta\Omega, \Omega + \Delta\Omega]$ (so called "signal bin") and approximate R by \tilde{R}

$$(2.13) \quad \tilde{R} = \frac{Q(\Omega, \Delta\Omega) - \Delta\Omega (S_o(\Omega - \Delta\Omega) + S_o(\Omega + \Delta\Omega))}{(S_o(\Omega - \Delta\Omega) + S_o(\Omega + \Delta\Omega))/2},$$

where

$$Q(\Omega, \Delta\Omega) = F(\Omega + \Delta\Omega) - F(\Omega - \Delta\Omega) = \frac{2}{\pi} \int_0^\infty K(\tau) \cos\Omega\tau \frac{\sin\Delta\Omega\tau}{\tau} d\tau.$$

This approximation of SNR coincides in general with one used in other papers on SR. Here, as it is usually done, $S_o(\omega)$ is assumed to be a sufficiently slowly varying function. Our experiments proved this fact.

To calculate SNR the stationary conditions (2.2) for the solution of (2.1) must be fulfilled. (As mentioned at the beginning of this section, the system (2.1) has a stationary solution.) Naturally, we can ensure this requirement rigorously only at infinite time. But the solution may already have good (for our aims, i.e., an error arising due to this reason is not greater than the other errors in the experiment) stationary properties at a certain time moment T_s after the beginning of SDE simulation. We checked the fulfilment of the conditions (2.2) for a solution of SDE (2.1) in our experiments by the calculation of $EX(s)$ and $K(\tau) = K(s, s + \tau)$ for various s and found that it is enough to take T_s equal to 3 periods of the applied periodic force in our case. We also found that $EX(s)$ is equal to zero, and below we write formulas omitting $EX(s)$.

Due to the fact that the system is simulated on a finite time interval $[0, T_s + T]$, we approximate $Q(\Omega, \Delta\Omega)$ and $S_o(\omega)$ by $Q_T(\Omega, \Delta\Omega)$ and $S_{oT}(\omega)$ correspondingly. Consequently, we calculate the following value

$$(2.14) \quad \tilde{R}_T = \frac{Q_T(\Omega, \Delta\Omega) - \Delta\Omega (S_{oT}(\Omega - \Delta\Omega) + S_{oT}(\Omega + \Delta\Omega))}{(S_{oT}(\Omega - \Delta\Omega) + S_{oT}(\Omega + \Delta\Omega))/2}$$

in our numerical experiments, which approximates \tilde{R} and, therefore, R . Note that we simulate the system (2.1) on the time interval $[0, T_s]$ to ensure the stationary properties (2.2) and on the time interval $[T_s, T_s + T]$ to calculate \tilde{R}_T .

The function $Q_T(\Omega, \Delta\Omega)$ in (2.14) is equal to

$$\begin{aligned} Q_T(\Omega, \Delta\Omega) &= \frac{2}{\pi} \int_0^T K(\tau) \cos\Omega\tau \frac{\sin\Delta\Omega\tau}{\tau} d\tau \\ &= \frac{2}{\pi} E \left[X_c(T_s) \int_{T_s}^{T_s+T} X_c(t) \cos\Omega(t - T_s) \frac{\sin\Delta\Omega(t - T_s)}{t - T_s} dt \right] \end{aligned}$$

and we calculate it as

$$(2.15) \quad Q_T(\Omega, \Delta\Omega) = \frac{2}{\pi} EX_c(T_s) Z(T_s + T)$$

where $Z(t)$ obeys the following subsidiary equation

$$dZ = X_c(t) \cos\Omega(t - T_s) \frac{\sin\Delta\Omega(t - T_s)}{t - T_s} dt, \quad Z(T_s) = 0$$

which we simulate together with the system (2.1) using the same method as described in Section 2.1.

The spectral function $F(\omega)$ can be rewritten as

$$F(\omega) = \frac{1}{\pi} \int_0^\infty K(\tau) \frac{\sin\omega\tau}{\tau} d\tau = \lim_{T \rightarrow \infty} \frac{1}{\pi} \int_0^T K(\tau) \left(\frac{1}{\tau} - \frac{1}{T} \right) \sin\omega\tau d\tau$$

because $\frac{1}{T} \int_0^T K(\tau) \sin\omega\tau d\tau$ goes to zero as T goes to infinity. Then, using the relation [22]

$$(2.16) \quad \int_0^T K(\tau) \left(1 - \frac{\tau}{T} \right) \cos\omega\tau d\tau = \frac{1}{2T} E \left| \int_{T_s}^{T_s+T} X_c(t) e^{i\omega(t-T_s)} dt \right|^2$$

we have

$$F(\omega) = \lim_{T \rightarrow \infty} \frac{1}{2\pi T} \int_0^\omega E \left| \int_{T_s}^{T_s+T} X_c(t) e^{i\tilde{\omega}(t-T_s)} dt \right|^2 d\tilde{\omega}$$

and

$$\tilde{S}(\omega) = \lim_{T \rightarrow \infty} \frac{1}{2\pi T} E \left| \int_{T_s}^{T_s+T} X_c(t) e^{i\omega(t-T_s)} dt \right|^2$$

The function $\tilde{S}(\omega)$ is exactly equal to $S_o(\omega)$ at the points $\omega \neq (2k-1)\Omega$, $k = 1, 2, \dots$ ³. Then, we can take the function $S_T(\omega)$

$$S_T(\omega) = \frac{1}{2\pi T} E \left| \int_{T_s}^{T_s+T} X_c(t) e^{i\omega(t-T_s)} dt \right|^2$$

instead of $S_{o_T}(\omega)$ on calculating \tilde{R}_T (see (2.14)) if $\Delta\Omega$ is sufficiently small and such that $S_T(\omega)$ has no sharp variations outside the intervals $((2k-1)\Omega - \Delta\Omega, (2k-1)\Omega + \Delta\Omega)$, $k = 1, 2, \dots$. We calculate $S_T(\omega)$ as

$$(2.17) \quad S_T(\omega) = \frac{1}{2\pi T} E \left(\hat{Y}_\omega^2(T_s + T) + \check{Y}_\omega^2(T_s + T) \right)$$

where $\hat{Y}_\omega(t)$ and $\check{Y}_\omega(t)$ obey the following equations

$$(2.18) \quad \begin{aligned} d\hat{Y}_\omega &= X_c(t) \cos \omega(t - T_s) dt, \\ d\check{Y}_\omega &= X_c(t) \sin \omega(t - T_s) dt, \\ \hat{Y}_\omega(T_s) &= \check{Y}_\omega(T_s) = 0. \end{aligned}$$

We take into account here that $X(t)$ is a process with real values. We simulate (2.18) together with the system (2.1) by the same method as described in Section 2.1.

Additionally to common errors (a method error and Monte Carlo error) arising in simulation of SDE by a weak method, we have errors on calculating \tilde{R} due to finite time of simulation.

The estimators $Q_T(\Omega, \Delta\Omega)$ and $S_T(\omega)$ are biased ones for $Q(\Omega, \Delta\Omega)$ and $S_o(\omega)$ (see, e.g., [25]) since the errors $\rho_{Q_T}(\Omega, \Delta\Omega) = Q(\Omega, \Delta\Omega) - Q_T(\Omega, \Delta\Omega)$ and $\rho_{S_T}(\omega) = S_o(\omega) - S_T(\omega)$ are usually not equal to zero. But taking enough large T , we can ensure a sufficient smallness of these errors. To prove the smallness in comparison with other errors arising in our experiments, we check a variation of \tilde{R}_T with growing T . We consider $T_s + T$ as enough big time for simulation if the variation of \tilde{R}_T with growing T is not greater than the other errors, e.g., as the Monte Carlo error. To check that taken time step h ensures the numerical integration error to be not greater than the other errors in our experiments, we carry out the repeated calculations of some points of \tilde{R}_T with the time step $h/2$.

The finiteness of time interval also produces loss of spectrum resolution [25], according to which we can calculate $S_T(\omega)$ only at $\omega = 2\pi k/T$, $k = 0, 1, 2, \dots$.

Because of time discretization, that we naturally use for numerical simulation of (2.1), the highest frequency (the Nyquist frequency), which is possible to pick out, is equal to

³Indeed, according to (2.6) and (2.4)

$$S_o(\omega) = \frac{1}{\pi} \int_0^\infty K_o(\tau) \cos \omega \tau d\tau = \frac{1}{\pi} \int_0^\infty \left[K(\tau) - 2 \sum_{k=1}^\infty \alpha_{2k-1} \cos(2k-1)\Omega\tau \right] \cos \omega \tau d\tau$$

Then, in the case of $\omega \neq (2k-1)\Omega$, $k = 1, 2, \dots$ we have

$$S_o(\omega) = \frac{1}{\pi} \lim_{T \rightarrow \infty} \left\{ \int_0^T K(\tau) \cos \omega \tau d\tau - \sum_{k=1}^\infty \alpha_{2k-1} \left[\frac{\sin((2k-1)\Omega + \omega)T}{(2k-1)\Omega + \omega} + \frac{\sin((2k-1)\Omega - \omega)T}{(2k-1)\Omega - \omega} \right] \right\}$$

Using the limits:

$$\int_0^T \frac{\tau}{T} K_o(\tau) \cos \omega \tau d\tau \rightarrow 0 \quad \text{and} \quad \int_0^T \left(1 - \frac{\tau}{T}\right) \cos \tilde{\omega} \tau d\tau \rightarrow 0 \quad \text{as} \quad T \rightarrow \infty$$

and (2.16), we obtain

$$S_o(\omega) = \frac{1}{\pi} \lim_{T \rightarrow \infty} \int_0^T K(\tau) \left(1 - \frac{\tau}{T}\right) \cos \omega \tau d\tau = \lim_{T \rightarrow \infty} \frac{1}{2\pi T} E \left| \int_{T_s}^{T_s+T} X_c(t) e^{i\omega(t-T_s)} dt \right|^2 = \tilde{S}(\omega)$$

at $\omega \neq (2k-1)\Omega$, $k = 1, 2, \dots$

$\omega_N = \pi/h$ [25], where h is a step of time discretization. Note that the time step h in our experiments is such that frequencies of the interesting range $[\Omega - \Delta\Omega, \Omega + \Delta\Omega]$ are much smaller than ω_N .

Remark 2.1. As mentioned above, we simulate values like $Ef(X(T_1))g(X(T_2))$ (e.g., $K(\tau)$ or $Q_T(\Omega, \Delta\Omega)$) by the weak method. But the existing theorems on weak convergence of a numerical method [15, 16, 17, 18, 19] were proved for calculating an expectation like $Ef(X(T))$. The proposition of Appendix gives us a right also to simulate $Ef(X(T_1))g(X(T_2))$ by weak methods.

Remark 2.2. One can see that our procedure of calculating SNR is a little bit different in comparison with the generally used one. The procedure usually contains the following steps (see, e.g., [4, 10, 11])

a) simulation of SDE solutions $X(t)$ by a mean-square method (as a rule, the mean-square Euler method);

b) obtained random trajectories $X(t)$ are considered as experimental statistical data, to which fast Fourier transform is applied to calculate a random spectrum, and by averaging a number of segments and samples of the random spectrum, $S_T(\omega)$ is found;

c) SNR is calculated on the base of $S_T(\omega)$ (α_1 is found as a square under $S_T(\omega)$ in a signal bin).

According to our procedure, we use a weak method, which gives us an opportunity to calculate the needed values with a large integration step (e.g., 0.1 in our experiments) in comparison with the steps (0.005, 0.002, etc.) taken in the previous works (see, e.g., [4, 10, 11]); we simulate both the investigated system and the values needed for the approximation \tilde{R}_T of SNR by the same numerical method. Due to its features, the proposed technique essentially saves CPU time providing a sufficiently high accuracy.

2.3. Simulation of phase shifts. Another important characteristic of SR is a phase lag (phase shift) between the applied periodic force and the response. The phase shift is a quantity of special interest in the context of condensed-matter physics since it is the phase shift that determines the absorption of the energy from the force [26]. It was found for one-dimensional systems (see, e.g., [27, 26]) that the phase shift also has a non-monotonic (extremal) behavior with noise increasing.

As mentioned at the beginning of this section, a solution $X(t)$ of (2.1) is a periodic one under any fixed initial phase φ . By the definition of periodic process (see (2.3)), we have

$$E[X(t)|\varphi = \varphi_o] = E[X(t + 2\pi/\Omega)|\varphi = \varphi_o]$$

Then, we can expand $E[X(t)|\varphi = \varphi_o]$ in the Fourier series:

$$E[X(t)|\varphi = \varphi_o] = \sum_{k=0}^{\infty} \beta_k \sin(k\Omega t + \varphi_o - \psi_k)$$

As is usual (see, e.g., [27, 26]), we are interesting in the value of the phase shift ψ_1 . It can be found as

$$(2.19) \quad \psi_1 = -\arctan(EZ_1(T_s + T)/EZ_2(T_s + T))$$

where $Z_1(t)$ and $Z_2(t)$ obey the following equations

$$(2.20) \quad \begin{aligned} dZ_1 &= X_c(t) \cos(\Omega t + \varphi) dt, \\ dZ_2 &= X_c(t) \sin(\Omega t + \varphi) dt, \\ Z_1(T_s) &= Z_2(T_s) = 0 \end{aligned}$$

Here T_s is a time moment, after which we suppose, as above, that $X(t)$ has already good stationary properties; T is equal to $2\pi k/\Omega$, $k = 1, 2, \dots$; the initial phase φ in (2.20)

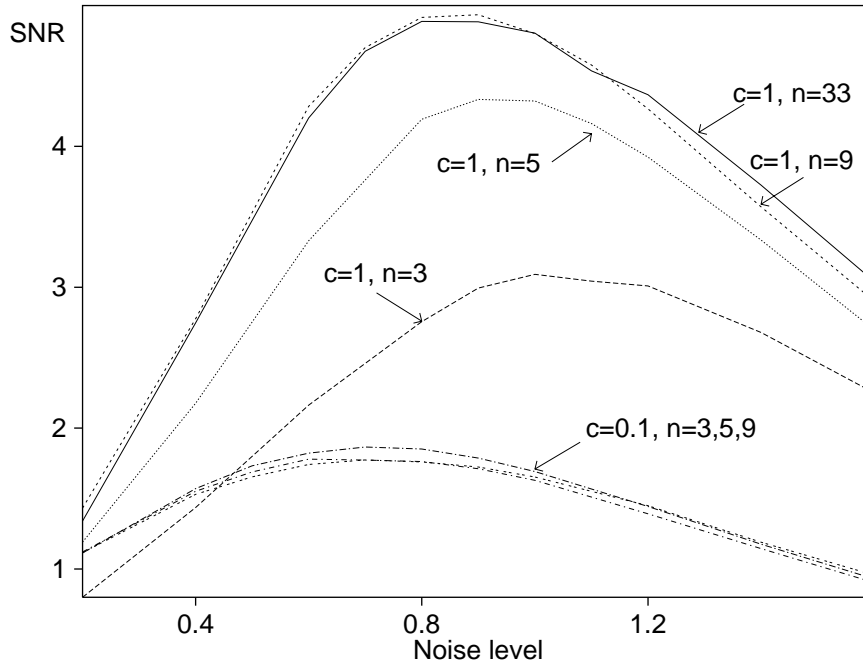


FIGURE 2. Signal-to-noise ratio versus noise level for the middle oscillators of the arrays (2.1) under the parameters: $a = 2.1078$, $b = 1.4706$, $A = 1.3039$, $\Omega = 0.7301$, $T_s = 6\pi/\Omega$, $T = 40\pi/\Omega$. The Monte Carlo error is less than 0.26.

is the same as in SDE (2.1) for $X(t)$ (we take it uniformly distributed as above). The equations (2.20) are also simulated by the weak method (2.7) of Section 2.1.

3. RESULTS OF NUMERICAL EXPERIMENT

To carry out our experiments, we take the parameters of the system (2.1) for array of noisy coupled oscillators just as in [10, 11]. They are $a = 2.1078$, $b = 1.4706$, $A = 1.3039$, $\Omega = 0.7301$. These values of parameters provide the operating regime just below the deterministic switching threshold so that in the absence of noise the oscillator is confined to a single well of the bistable potential, but small noise can induce significant hopping between wells [10]. As mentioned in [10, 11], these parameter values are not special and the features of AESR can also be observed at another set of parameters. The differential equations of Section 2, needed for calculating SNR and phase shifts, are simulated by the weak method (2.7) with the time step $h = 0.1$, with exception of the curves of Figure 5 where we use $h = 0.2$ for noise level $\varepsilon = 0 \div 0.5$ (note that the main SR effect on the phase shifts is namely in this range of ε). To calculate the needed mean values, we simulate N_r independent realizations of a solution $X(t)$ of (2.1). We take N_r equal to 4000 in all our experiments, excepting the curve of Figure 5 under $c = 0$ and $\varepsilon = 0.02 \div 0.15$ for which $N_r = 10000$. All the errors arising in our experiments are smaller or comparable with the Monte Carlo error (we control the errors by the repeated calculations of some points of SNR and phase shifts under a smaller step h , greater N_r , and greater T). To simulate the needed random variables, we use random generators of Ref. [28].

Figures 2, 3 and 4 present the SNR behavior. SNR is a non-monotonic (extremal) function both of noise and of coupling. If the extremal behavior with noise increasing is a common feature of all systems connected with the SR phenomenon, the SNR extremal behavior with growing of coupling is attributable to the AESR phenomenon. These results coincide with ones of [10, 11]. We also come to the same conclusion as authors of the previous papers that increasing of the array length n improves SNR. However, according

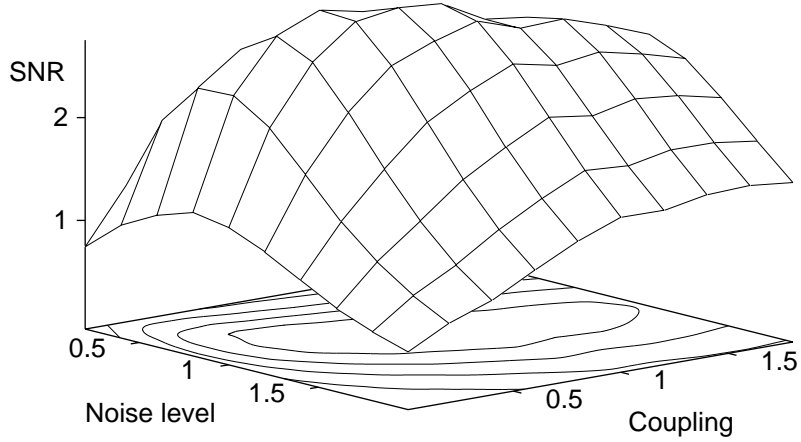


FIGURE 3. Signal-to-noise ratio versus noise level ε and coupling c for the middle oscillator of the array of three oscillators (2.1). The parameters are the same as in Figure 2. The Monte Carlo error is less than 0.17.

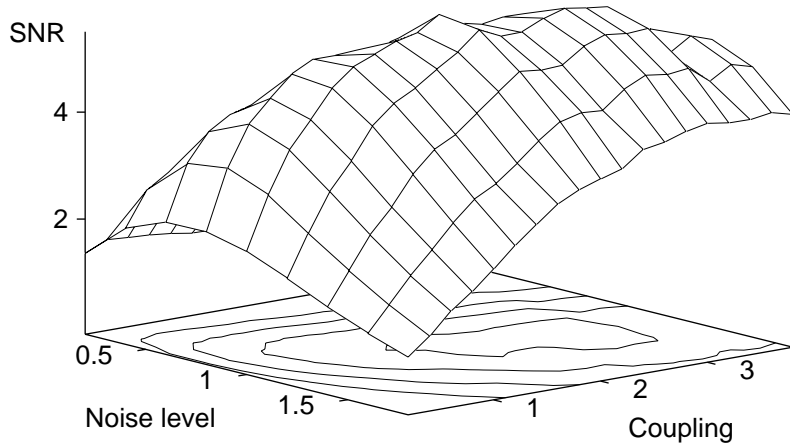


FIGURE 4. Signal-to-noise ratio versus noise level ε and coupling c for the middle oscillator of the array of nine oscillators. The parameters are the same as in Figure 2. The Monte Carlo error is less than 0.3.

to Figure 2, there is a length n_* of the array such that further increasing of the array length n does not lead to improving SNR at each fixed coupling c .

Figures 5 and 6 show the extremal behavior of the phase shifts. Maxima of phase shifts appear at a lower noise level in comparison with the noise level corresponding to the SNR maxima. This fact corresponds with the results of Ref. [27] on a single oscillator.

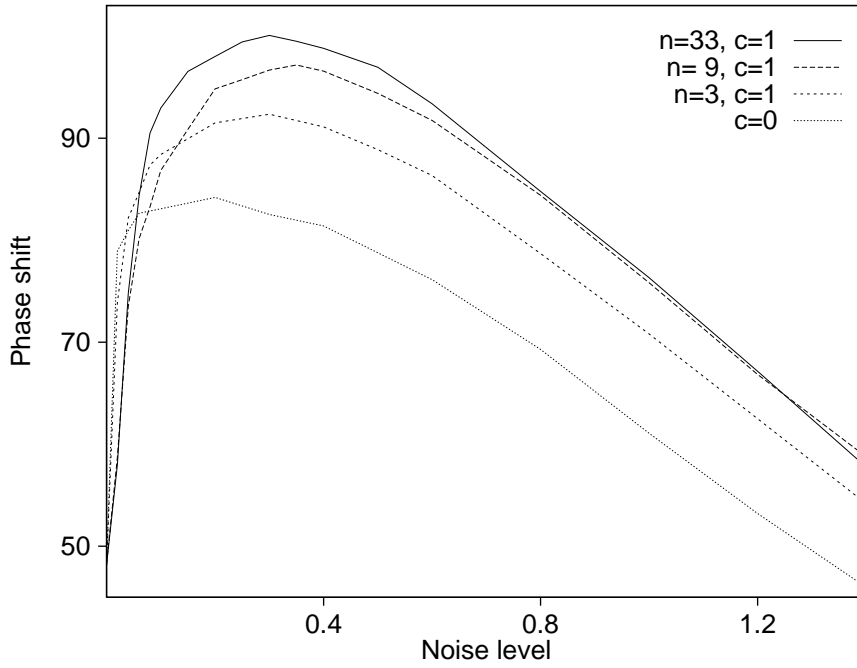


FIGURE 5. The phase shifts ψ_1 of the middle oscillators from the corresponding arrays described by (2.1). The parameters are the same as in Figure 2 (with exception of $T = 8\pi/\Omega$). The Monte Carlo error is less than 1.7

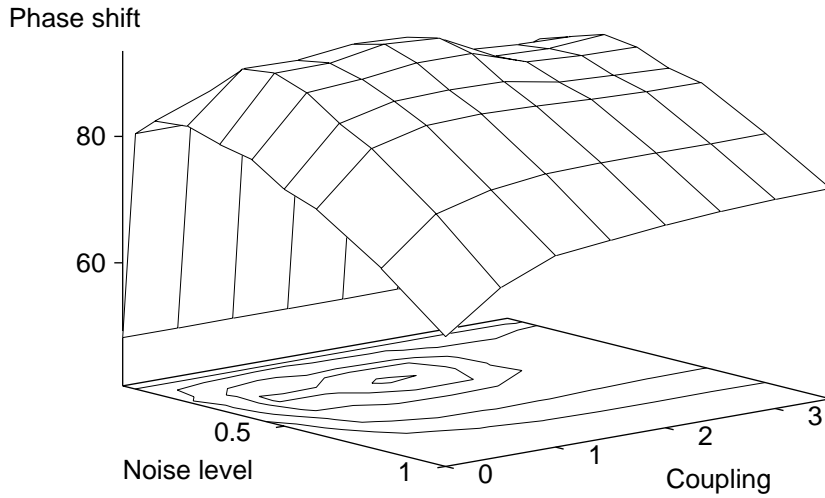


FIGURE 6. The phase shifts ψ_1 versus noise level ε and coupling c of the middle oscillator from the array of three oscillators. The parameters are the same as in Figure 5. The Monte Carlo error is less than 1.9.

The phase shift is also a non-monotonic function of coupling in the case of noisy coupled oscillators (see Figure 6). Increasing of the array length n improves the effect just as it affects SNR (see Figure 5).

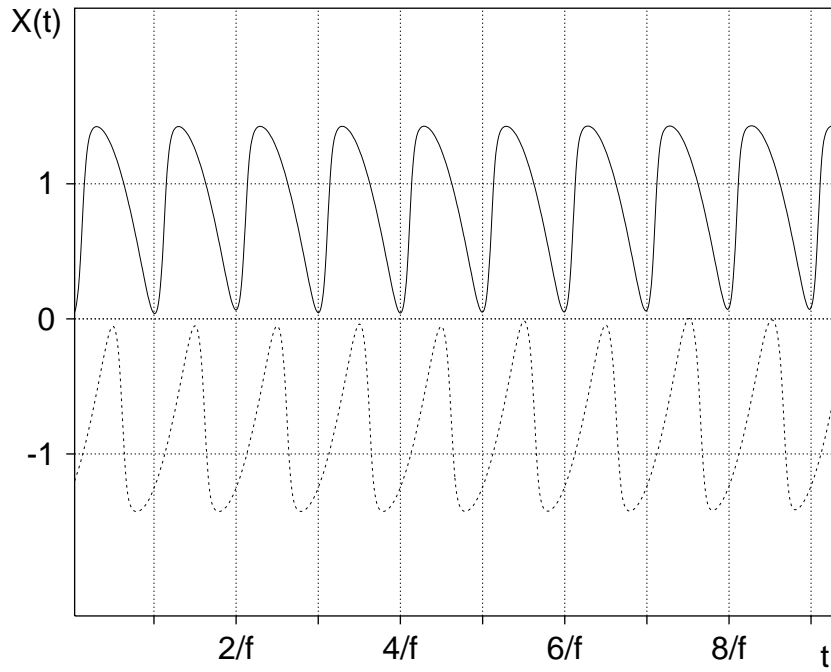


FIGURE 7. A sample trajectories of the first (dotted line) and the middle (solid line) oscillators of the array of 33 oscillators (2.1) under $c = 1.8$ and $\varepsilon = 0.001$. Other parameter values are the same as in Figure 2.

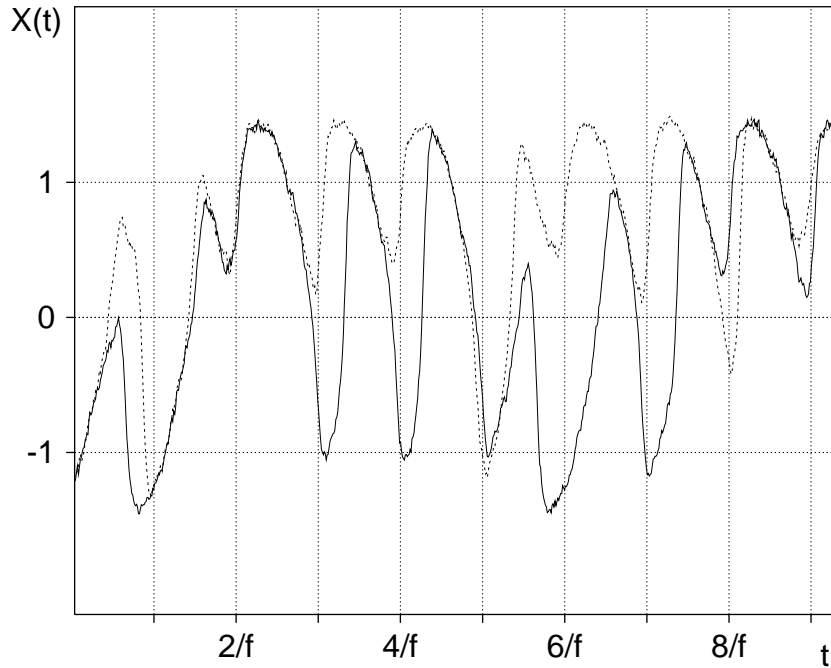


FIGURE 8. A sample trajectories of the first (dotted line) and the middle (solid line) oscillators of the array of 33 oscillators under $c = 1.8$ and $\varepsilon = 0.1$. Other parameter values are the same as in Figure 2.

Another interesting feature of the AESR phenomenon is known as a spatiotemporal synchronization [10, 11, 13]. The spatiotemporal synchronization means within the AESR context that an oscillator of the array changes its temporal order synchronously with other elements of the array with noise increasing. Note that such a coherence behavior of oscillators occurs even in the absence of coupling, $c = 0$, (see [14]), and one can also

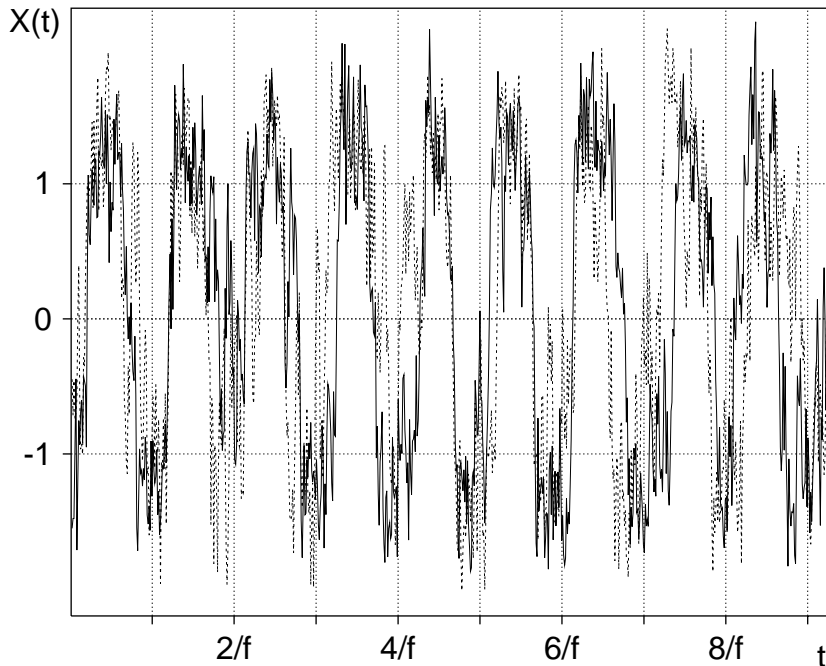


FIGURE 9. A sample trajectories of the first (dotted line) and the middle (solid line) oscillators of the array of 33 oscillators under $c = 1.8$ and $\varepsilon = 1.5$. Other parameter values are the same as in Figure 2.

observe a synchronous behavior of various sample trajectories of a single oscillator under a certain noise level. As mentioned in [14] and observed in our experiments, the effect of spatiotemporal synchronization is improved by increasing the coupling. The spatiotemporal synchronization was shown through the observation of trajectories of oscillators and by an occupancy function in the previous papers. Here we demonstrate the synchronous behavior of the array elements by the trajectory analysis (compare Figures 7, 8, and 9). We simulate sample trajectories for (2.1) by the mean-square Runge-Kutta method with error $O(h^4 + \varepsilon^2 h^{3/2})$ of Ref. [29]. At a low noise level (Figure 7) the array elements oscillate during a long time around one of two stable states depending on the initial conditions. Random switching appears more often with noise increasing and the array loses its temporal order (Figure 8). At a certain noise level (Figure 9), which is close to the level corresponding to the SNR maximum, oscillators live together approximately 1/2-period of the applied periodic force in one well of the bistable potential and 1/2-period in another one, the spatiotemporal order is formed. Naturally, the order is corrupted under a higher noise level. Note that we observe the sample trajectories after the time moment T_s (i.e., $t = 0$ of these figures corresponds with T_s).

4. APPENDIX.

Definition 4.1. A function $f(x)$ belongs to the class \mathcal{F} , $f \in \mathcal{F}$, if constants $K > 0$ and $\alpha \geq 0$ are such that the inequality

$$(4.1) \quad |f(x)| \leq K(1 + |x|^\alpha)$$

is fulfilled for any $x \in \mathbb{R}^n$.

Note that the same letter K for various constants and the same notation $K(x)$ for various functions of the class \mathcal{F} are used in the estimates below.

Proposition 4.1. Let us consider

- (1) a system of stochastic differential equations, for which we assume that

- its coefficients are continuous, satisfy the Lipschitz condition and belong to the class \mathcal{F} together with their partial derivatives up to a sufficiently high order, and there are imposed additional restrictions on the coefficients such that the solution $X(t)$, $X(t_0) = X_o$, exists on the whole time interval $t \in [t_o, T]$; ⁴

- the moments $E|X(t)|^m$ exist for a sufficiently large number m and are uniformly bounded with respect to $t \in [t_o, T]$; ⁵

(2) a method $X_k = \bar{X}(t_k)$, $k = 0, 1, \dots, N$, $\bar{X}(t_o) = X_o$, for which we assume that

- it approximates the solution $X(t)$ of the system in weak sense with the error

$$(4.2) \quad |Ef(X_{t_o, X_o}(t_N)) - Ef(\bar{X}_{t_o, X_o}(t_N))| \leq K(X_o) h^p$$

where $p > 0$; $h = t_i - t_{i-1}$, $i = 1, \dots, N$, is a step of discretization of the time interval $[t_o, T]$, $t_N = T$; $f(x), K(x) \in \mathcal{F}$;

- the moments $E|X_k|^m$ exist for a sufficiently large number m and are uniformly bounded with respect to N , $k = 0, 1, \dots, N$.

Then for any $N_2 \geq N_1$

$$(4.3) \quad |Ef(X_{t_o, X_o}(t_{N_1}))g(X_{t_o, X_o}(t_{N_2})) - Ef(\bar{X}_{t_o, X_o}(t_{N_1}))g(\bar{X}_{t_o, X_o}(t_{N_2}))| \leq K h^p$$

where $f(x), g(x) \in \mathcal{F}$, and the constant K depends on X_o and t_{N_2} .

Proof. Let $t_{N_1} = T_1$, $t_{N_2} = T_2$. The inequality (4.3) can be rewritten as

$$(4.4) \quad \begin{aligned} \rho &= |Ef(X_{t_o, X_o}(T_1))g(X_{t_o, X_o}(T_2)) - Ef(\bar{X}_{t_o, X_o}(T_1))g(\bar{X}_{t_o, X_o}(T_2))| \\ &= |[Ef(\bar{X}_{t_o, X_o}(T_1))g(X_{T_1, \bar{X}(T_1)}(T_2)) - Ef(\bar{X}_{t_o, X_o}(T_1))g(\bar{X}_{T_1, \bar{X}(T_1)}(T_2))] \\ &\quad + [Ef(X_{t_o, X_o}(T_1))g(X_{t_o, X_o}(T_2)) - Ef(\bar{X}_{t_o, X_o}(T_1))g(X_{T_1, \bar{X}(T_1)}(T_2))]| \\ &\leq |E[f(\bar{X}_{t_o, X_o}(T_1))E\{g(X_{T_1, \bar{X}(T_1)}(T_2)) - g(\bar{X}_{T_1, \bar{X}(T_1)}(T_2)) | \bar{X}(T_1)\}]| \\ &\quad + |E[f(X_{t_o, X_o}(T_1))E\{g(X_{t_o, X_o}(T_2)) | X(T_1)\}]| \\ &\quad - E[f(\bar{X}_{t_o, X_o}(T_1))E\{g(X_{T_1, \bar{X}(T_1)}(T_2)) | \bar{X}(T_1)\}]| \end{aligned}$$

According to the conditions of the proposition, we obtain for the first term of (4.4):

$$\begin{aligned} \rho_1 &= |E[f(\bar{X}_{t_o, X_o}(T_1))E\{g(X_{T_1, \bar{X}(T_1)}(T_2)) - g(\bar{X}_{T_1, \bar{X}(T_1)}(T_2)) | \bar{X}(T_1)\}]| \\ &\leq E[|f(\bar{X}_{t_o, X_o}(T_1))| \cdot K(\bar{X}(T_1))h^p] \leq Kh^p \end{aligned}$$

Let us involve the function

$$u(s, t) = Eg(X_{s, x}(T_2))$$

Due to the conditions (1) of the proposition, the function u has partial derivatives with respect to x up to a sufficiently high order, and the function u and its derivatives belong to the class \mathcal{F} [30] (see Theorem 1 of § 8 and its Corollary 1⁶). The function $u(s, x)$ uniformly, with respect to $s \in [t_o, T_2]$, satisfies such an inequality as (4.2).

Now the second term of (4.4) can be rewritten as

$$\begin{aligned} \rho_2 &= |E[f(X_{t_o, X_o}(T_1))E\{g(X_{t_o, X_o}(T_2)) | X(T_1)\}]| \\ &\quad - E[f(\bar{X}_{t_o, X_o}(T_1))E\{g(X_{T_1, \bar{X}(T_1)}(T_2)) | \bar{X}(T_1)\}]| \\ &= |E[f(X_{t_o, X_o}(T_1))u(T_1, X_{t_o, X_o}(T_1))] - E[f(\bar{X}_{t_o, X_o}(T_1))u(T_1, \bar{X}_{t_o, X_o}(T_1))]| \end{aligned}$$

⁴One can check the fulfilment of this assumption for the system (2.1) by Theorem 4.1 of Ch. 3, § 4 [21].

⁵The fulfilment of this assumption for the system (2.1) follows from the results of Ch. 3, § 4 [21] taking into account that in our case the Lyapunov function $V = (|x|^2 + 1)^{m/2}$ satisfies conditions of Theorem 4.1 of Ch.3, § 4 [21] for any $m > 0$.

⁶Conditions of this theorem contain the requirement on the growth of the SDE coefficients to be not greater than linear. But its proof uses only the boundedness of sufficiently high moments of SDE solution (see the conditions (1) of our proposition).

Involving the function $\psi(x) = f(x)u(x)$, $\psi(x) \in \mathcal{F}$, and using (4.2), we obtain

$$\rho_2 \leq Kh^p$$

So, we have

$$\rho \leq \rho_1 + \rho_2 \leq Kh^p$$

■

Remark 4.1. The conditions of the proposition correspond with the existing theorems on weak convergence of numerical methods for SDE [15, 16, 17, 18]. It is also possible to prove the similar proposition for the methods of Ref. [19], where errors have the form $O(h^p + \varepsilon^\alpha h^q)$.

ACKNOWLEDGMENTS

The author acknowledges valuable constant discussions with Professor G.N.Milstein and is grateful to the Alexander von Humboldt Foundation for support of this work through a research fellowship.

REFERENCES

- [1] R.Benzi, A.Sutterra, and A.Vulpiani, *The mechanism of stochastic resonance* J.Phys. A v.14 (1981), L.453-L457
- [2] B.McNamara, K.Wiesenfeld, and R.Roy, *Observation of stochastic resonance in a ring laser* Phys.Rev.Lett. v.60 (1988), pp.2626-2629
- [3] A.Longtin, A.Bulsara, D.Pierson, and F.Moss, *Bistability and the dynamics of periodically forced sensory neurons* Biol.Cybern. v.70 (1994), pp.569-578; A.R.Bulsara, T.C.Elston, C.R.Doering, S.B.Lowen, and K.Lindenberg, *Cooperative behavior in periodically driven noisy integrate-fire models of neuronal dynamics* Phys.Rev.E v.53 (1996), pp.3958-3969
- [4] A.Longtin, *Synchronization of the stochastic Fitzhugh-Nagumo equations to periodic forcing* in [7] pp. 835-846
- [5] A.D.Hibbs, A.L.Singsaas, E.W.Jacobs, A.R.Bulsara, J.J.Bekkendahl, and F.Moss, *Stochastic resonance in a superconducting loop with a Josephson function* J.Appl.Phys. v.77 (1995), pp. 2582-2590
- [6] Proceedings of the NATO Advanced Research Workshop on Stochastic Resonance in Physics and Biology, J.Stat.Phys. v.70 (1993), No 1/2
- [7] Proceedings of the International Workshop "Fluctuations in Physics and Biology: Stochastic Resonance, Signal Processing and Related Phenomena", Nuovo Cimento Della Societa Italiana di Fisica D v.17 (1995), No 7/8
- [8] F.Moss, *Stochastic resonance: From the ice ages to the monkey's ear* in "Contemporary problems in statistical physics" Ed. G.H.Weiss, SIAM, Philadelphia, 1994, pp. 205-253
- [9] <http://www.pg.infn.it/sr/>
- [10] J.F.Lindner, B.K.Meadows, W.L.Ditto, M.E.Inchiosa, and A.R.Bulsara, *Array enhanced stochastic resonance and spatiotemporal synchronization* Phys.Rev.Lett. v.75 (1995), pp. 3-6
- [11] J.F.Lindner, B.K.Meadows, W.L.Ditto, M.E.Inchiosa, and A.R.Bulsara, *Scaling laws for spatiotemporal synchronization and array enhanced SR* Phys.Rev.E v.53 (1996), pp. 2081-2086
- [12] M.E.Inchiosa and A.R.Bulsara, *Nonlinear dynamic elements with noisy sinusoidal forcing: Enhancing response via nonlinear coupling* Phys.Rev.E v.52 (1995), pp.327-339; Hu Gang, H.Haken, and Xie Fagen, *Stochastic resonance with sensitive frequency dependence in globally coupled continuous system* Phys.Rev.Lett. v.77 (1996), pp.1925-1928
- [13] M.Löcher, G.A.Johnson, and E.R.Hunt, *Spatiotemporal stochastic resonance in a system of coupled diode resonators* Phys.Rev.Lett. v.77 (1996), pp.4698-4701
- [14] A.Neiman and L.Schimansky-Geier, *Stochastic resonance in two coupled bistable systems* Phys.Lett. A v.197 (1995), pp. 379-386
- [15] G.N.Milstein, *A method of second-order accuracy integration of stochastic differential equations* Theor.Prob.Appl. v.23 (1978), pp.396-401; *Weak approximation of solutions of systems of stochastic differential equations* Theor.Prob.Appl. v.30 (1985), pp.750-766
- [16] G.N.Milstein, *Numerical Integration of Stochastic Differential Equations* (Ural Univ.Press, Sverdlovsk, 1988; Kluwer Academic Publishers, 1995)

- [17] E.Pardoux and D.Talay, *Discretization and simulation of stochastic differential equations* Acta Appl.Math. v.3 (1985), pp. 23-47
- [18] P.E.Kloeden and E.Platen, *Numerical Solution of Stochastic Differential Equations* (Springer-Verlag, Berlin, 1992)
- [19] G.N.Milstein and M.V.Tretyakov, *Weak approximation for stochastic differential equations with small noises*, WIAS Preprint No. 123, Berlin, 1994; *Numerical methods in the weak sense for stochastic differential equations with small noise* SIAM J.Numer.Anal. (1997), in print
- [20] R.Bartussek, P.Hänggi, and P.Jung, *Stochastic resonance in optical bistable systems* Phys.Rev.E v.49 (1994), pp.3930-3939
- [21] R.Z.Hasminski, *Stability of Differential Equations under Random Perturbations of their Parameters* (Nauka, Moscow, 1969); English edition: Sijthoff & Noordhoff, 1980
- [22] A.D.Wentzell, *A Course in the Theory of Random Processes* (Mc Graw-Hill, N.Y., 1981)
- [23] R.L.Stratonovich, *Topics in the Theory of Random Noise* (Gordon&Breach, N.Y., 1963)
- [24] B.McNamara and K.Wiesenfeld, *Theory of stochastic resonance* Phys.Rev. A. v.39 (1989), pp.4854-4869
- [25] D.B.Percival and A.T.Walden, *Spectral Analysis for Physical Applications* (Cambridge Univ.Press, 1993, Cambridge); J.S.Bendat and A.G.Piersol, *Random Data. Analysis and Measurement Procedures* (John Wiley & Sons, 1986, N.Y.)
- [26] M.I.Dykman, D.G.Luchinsky, R.Mannella, P.V.E.McClintock, N.D.Stein, and N.D.Stocks, *Stochastic resonance in perspective* in [7] pp.661-683
- [27] M.I.Dykman, R.Mannella, P.V.E.McClintock, and N.G.Stocks, *Phase shifts in stochastic resonance* Phys.Rev.Lett. v.68 (1992), pp.2985-2988
- [28] W.H.Press, S.A.Teukolsky, W.T.Vetterling, and B.P.Flannery, *Numerical Recipes in Fortran: The Art of Scientific Computing* (Cambridge Univ. Press, Cambridge, 1992)
- [29] G.N.Milstein and M.V.Tretyakov, *Mean-square numerical methods for stochastic differential equations with small noises*, SIAM J.Sci.Comp. (1997), in print
- [30] I.I.Gihman and A.V.Scorohod, *Stochastic Differential Equations* (Naukova Dumka, Kiev, 1968); English edition: Springer, 1972